ACS POLYMERS Au
AN OPEN ACCESS JOURNAL OF THE AMERICAN CHEMICAL SOCIETY

pubs.acs.org/polymerau

Article

Enhanced Dielectric Strength and Capacitive Energy Density of Cyclic Polystyrene Films

Maninderjeet Singh, Mei Dong, Wenjie Wu, Roushanak Nejat, David K. Tran, Nihar Pradhan, Dharmaraj Raghavan, Jack F. Douglas, Karen L. Wooley, and Alamgir Karim*

Cite This: ACS Polym. Au 2022, 2, 324–332

Read Online

ACCESS | Metrics & More | Article Recommendations | Supporting Information

ABSTRACT: The maximum capacitive energy stored in polymeric dielectric capacitors, which are ubiquitous in high-power-density devices, is dictated by the dielectric breakdown strength of the dielectric polymer. The fundamental mechanisms of the dielectric breakdown, however, remain unclear. Based on a simple free-volume model of the polymer fluid state, we hypothesized that the free ends of linear polymer chains might act as "defect" sites, at which the dielectric breakdown can initiate. Thus, the dielectric breakdown strength of cyclic polymers should exhibit enhanced stability in comparison to that of their linear counterparts having the same composition and similar molar mass. This hypothesis is supported by the ∼50% enhancement in the dielectric breakdown strength and ∼80% enhancement in capacitive energy density of cyclic polystyrene melt films in comparison to corresponding linear polystyrene control films. Furthermore, we observed that cyclic polymers exhibit a denser packing density than the linear chain melts, an effect that is consistent with and could account for the observed property changes. Our work demonstrates that polymer topology can significantly influence the capacitive properties of polymer films, and correspondingly, we can expect polymer topology to influence the gas permeability, shear modulus, and other properties of thin films dependent on film density.

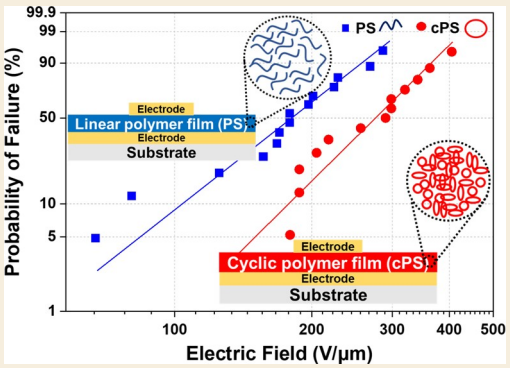

KEYWORDS: *Polymeric dielectric capacitors, Cyclic polymers, Ring polymers, Capacitive energy storage, Dielectric breakdown, Free volume, Chain-ends, Polymer films, Enhancing capacitive energy density*

INTRODUCTION

The ever-growing demand for clean, sustainable, and green energy along with the need for powerful futuristic devices necessitate innovation for increasing the energy density and efficiency of energy storage devices.[1] Among the various energy storage devices, dielectric capacitors[2−9] are promising candidates for high-power-density pulsed power devices due to their capability of ultrafast discharge (on the order of microseconds)[10] of stored energy. Because of their high power density, dielectric capacitors have found applications in microelectronics, medical devices, electric vehicles, aircraft, military equipment, consumer electronics, lasers, and the power industry.[8] Dielectric capacitors can be either ceramic-based[4] or polymer-based,[11−13] depending on the type of application. Polymer-based dielectric capacitors have the advantages of flexibility,[14] high dielectric strength, graceful failure, easy processability, and a low loss of stored energy over their ceramic counterparts, making them desirable for advanced applications that demand high power and energy density.[9] Although the power density of dielectric capacitors is the highest among other energy storage devices, dielectric capacitors suffer from much lower energy density as compared to supercapacitors and batteries.[1,8,9]

The maximum energy density (U) in a dielectric material is a function of the dielectric permittivity (or polarizability) (ε_r) and the maximum electric field (E_{BD}) that can be applied to the dielectric without degrading the dielectric material.[9] Depending on the relation between the permittivity and the electric field, the dielectrics (ceramics as well as polymers) can be classified as linear, paraelectric, ferroelectric, relaxor ferroelectric, and antiferroelectric.[8,9,12] The linear dielectrics (such as biaxially oriented polypropylene) have the lowest losses among these dielectrics, thus making them the material of choice for capacitive energy storage. The maximum energy density of linear dielectrics can be described by the relation

$$U_{max} = \frac{1}{2}\varepsilon_0\varepsilon_r E_{BD}^2 \quad (1)$$

Received: April 8, 2022
Revised: June 7, 2022
Accepted: June 7, 2022
Published: June 23, 2022

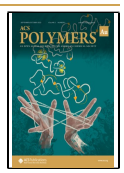

Scheme 1. Synthesis of Linear Polystyrene (Linear-PS-Br) (1) and Following Synthetic Modifications to Create Cyclic Polystyrene (cPS) (3), According to Literature Procedures[45]

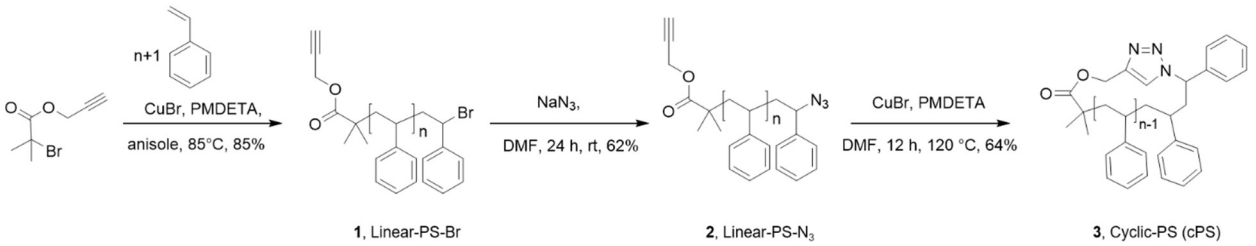

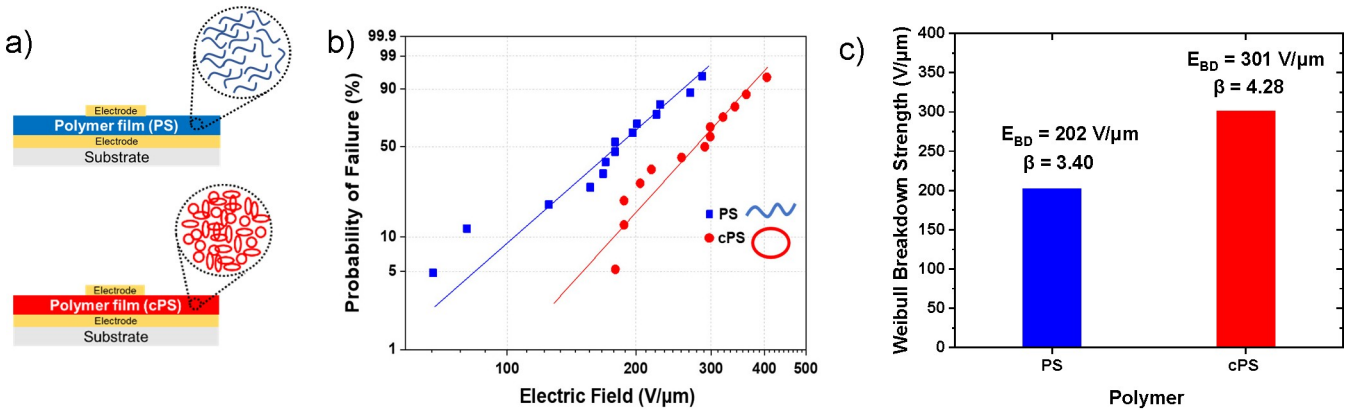

Figure 1. (a) Schematics of linear polystyrene (PS) and cyclic polystyrene (cPS) films used as dielectric capacitors in this study. (b) Weibull failure plots of linear polystyrene (PS) and cyclic polystyrene (cPS). (c) Weibull breakdown strength (E_{BD}) for PS and cPS. The Weibull breakdown strength is ∼50% higher for cPS as compared to the PS.

where U_{max} is the maximum energy density, ε_0 is the absolute permittivity, ε_r is the relative permittivity, and E_{BD} is the dielectric strength of the material, due to the independence of ε_r on the electric field. Thus, the maximum energy density of a linear dielectric depends quadratically on the maximum dielectric strength. Hence, increasing the dielectric strength should substantially increase the capacitive energy density of the dielectric capacitors. The dielectric strength and hence the capacitive energy density enhancement have been shown using nanofillers[15−17] in nanocomposites,[18−21] multilayered architectures,[22,23] and so on. To enhance the dielectric strength of pristine polymeric dielectrics, the fundamental mechanisms of dielectric breakdown in polymers should be taken into consideration. The free-volume theory of dielectric breakdown postulated by Artbauer demonstrates that the electrons accelerate in the free volume present in the polymer at high electric fields, resulting in the dielectric breakdown.[24] As such, strategies to decrease the free volume in the polymeric dielectric should enhance the dielectric strength and the capacitive energy density of the linear polymeric dielectrics. In our recent studies,[25,26] we showed that the dielectric strength increases by increasing chain-end separations in block-copolymer-based dielectric films.

Cyclic polymers are a class of polymers that do not possess chain-ends.[27−30] The syntheses and high-purity separation of cyclic polymers in recent years have been enabled by the advances in synthetic polymer chemistry.[27] Due to the lack of chain-ends in cyclic polymers, the cyclic polymers have properties that are different from their linear chain counterparts. Observations have already revealed property changes including power-law stress relaxation,[31] different pharmacokinetics and biodistribution,[32] different gel properties,[33] weaker molar mass dependence of the glass transition and glass fragility effects,[34,35] unique thermal transition behavior,[36] dewetting stability,[37,38] different crystallization kinetics,[39] different diffusion kinetics,[40] and so on. Given the fact that chain-ends are absent in cyclic polymers, we might speculate, from a free volume[41] viewpoint, that the dielectric strength and the capacitive energy density of cyclic polymers may be enhanced compared to their linear chain counterparts.

In this work, we show that the films prepared from cyclic polystyrene (cPS) indeed exhibit a highly enhanced dielectric (breakdown) strength and capacitive energy density as compared to the films prepared from linear polystyrene (PS) that have similar molar mass and dispersity. The dielectric strength of cPS shows ∼50% enhancement over that of PS, which translates to an ∼80% increase in the maximum capacitive energy density. The increase in the dielectric strength is tentatively attributed to the absence of chain-ends for cPS, relative to those of the linear polymer controls, which act as nucleation sites for the dielectric breakdown in polymer dielectric materials. The overall enhanced packing efficiency of cyclic polymer melts in comparison to their linear chain counterparts is another contributing factor for the property enhancements.[42] Although we have used a low dielectric strength (E_{BD}) polymer, i.e., polystyrene ($E_{BD} \approx 200$ V/μm), for proof-of-concept demonstration of enhancement of dielectric strength by chain-end elimination, recent advances in the polymer chemistry for synthesizing a number of cyclic polymers[30,36,43,44] should enable the extension of these results to other high-dielectric strength polymers as well.

RESULTS AND DISCUSSION

Cyclic polystyrene was produced in three steps through atom transfer radical polymerization, followed by nucleophilic

https://doi.org/10.1021/acspolymersau.2c00014
ACS Polym. Au 2022, 2, 324−332

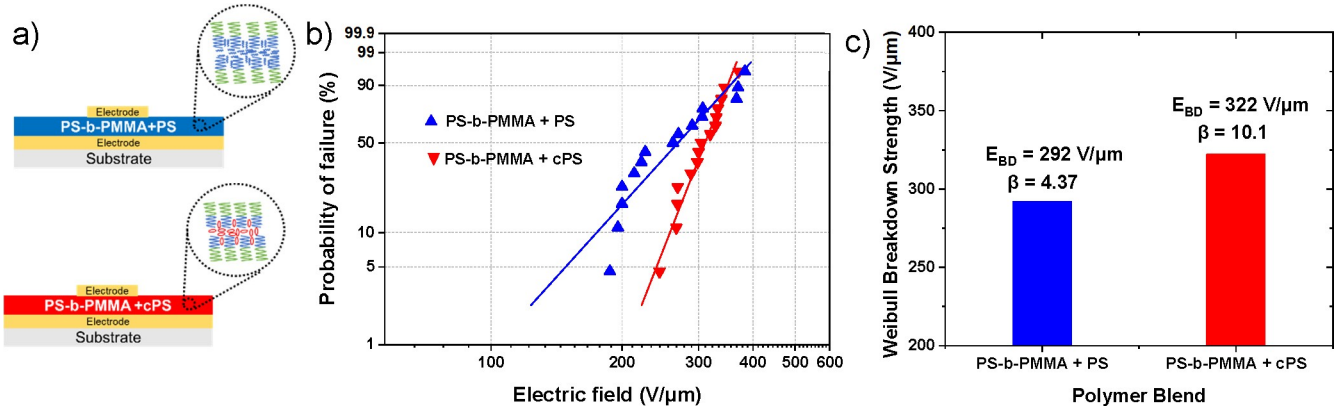

Figure 2. (a) Schematics of the block copolymer (polystyrene-*block*-poly(methyl methacrylate)) (PS-*b*-PMMA, 19.1-*b*-17.5 kDa) and homopolymer (PS or cPS, 6 kDa) blends used as dielectric capacitors. (b) Weibull failure plots of the PS-*b*-PMMA + PS blend and PS-*b*-PMMA + cPS blend. (c) Weibull breakdown strength (E_{BD}) for the PS-*b*-PMMA + PS blend and PS-*b*-PMMA + cPS blend. The Weibull breakdown strength of the cPS blend is ∼10% higher than that of PS blends, despite only 10% addition of the homopolymer (linear and cyclic) in the blend.

displacement and then ring-closure cyclization, following the procedure developed by Laurent and Grayson[45] as shown in Scheme 1. Using a propargyl-functionalized initiator, atom transfer radical polymerization of styrene afforded the linear polystyrene precursor (**1**) with terminal alkyne and bromide chain-ends. The resulting polymer **1** was then allowed to undergo a reaction with NaN_3 in dimethylformamide to convert the bromide chain-end to an azido chain-end and generate polymer **2**. Finally, the cyclic polystyrene **3** was synthesized by copper(I)-catalyzed azide−alkyne cycloaddition under dilute conditions, i.e., slow addition of **2** via syringe pump to a solution of the catalyst over the 12 h duration of the cyclization step, in order to suppress intermolecular chain−chain coupling.[45,46]

Cyclization of **2** was confirmed by several qualitative and quantitative characterizations. As presented in Supporting Information Figure S1c, a distinguishable peak shift from the short retention time (22.1 min) to the long retention time (22.5 min) between the size exclusion chromatography (SEC) profiles of **2** and **3** was observed, which indicated the formation of a more compact macromolecular structure upon cyclization. Both SEC traces show high-molar-mass shoulders (at slightly shorter retention times), which did not become more pronounced following the alkyne−azide click reaction, suggesting limited intermolecular chain−chain coupling events. Within the accuracy and resolution capabilities of ^{1}H NMR spectroscopy, the transformation of the alkyne and azide groups to the triazole was supported by downfield shifts of both the terminal methylene and benzylic protons upon cyclization (Supporting Information Figure S1b). In addition, the molar mass and dispersity of **3** were maintained the same as linear precursor **2**, which was confirmed by MALDI-TOF mass spectrometry (Supporting Information Figure S2).

The dielectric strengths of drop-cast and annealed (80 °C for 15 h) films of cPS vs. PS (6 kDa) are shown in Figure 1a−c. The Weibull dielectric (breakdown) strengths[25] are calculated using two-parameter Weibull statics described as

$$P(E) = 1 - \exp\left[-\left(\frac{E}{E_{BD}}\right)^{\beta}\right] \quad (2)$$

where $P(E)$ is the cumulative probability of dielectric failure, E is the measured dielectric breakdown strength, E_{BD} is the Weibull dielectric strength, i.e., dielectric strength at 63% of the probability of failure, and β is the shape factor, which represents the reliability of the breakdown data. The Weibull breakdown strength of cPS is ∼50% higher than that of PS for similar molar masses (6 kDa). The enhancement of the breakdown strength in cPS most likely stems from the absence of chain-end associated free volume in the cPS compared to PS polymer films.

According to the free-volume theory of dielectric breakdown developed by Artbauer,[24] the free volume present in the polymer films contributes to the electron acceleration, thus causing dielectric failure. The free volume per polymer chain in the PS polymer films can be modeled as

$$V_f^l = nV_c^l + 2V_e \quad (3)$$

where V_f^l is the free volume per polymer chain in the linear polymer films, n is the number of repeat units, V_c^l is the chain packing associated free volume per repeat unit, and V_e is the chain-end associated free volume per chain. Similarly, for the cyclic polymer films

$$V_f^c = nV_c^c \quad (4)$$

V_f^c is the free volume per chain in the cyclic polymer films, n is the number of repeat units, and V_c^c is the chain packing associated free volume per repeat unit. Given that the chain-end associated free volume does not exist in the cyclic polymer melts, we may expect their enhanced stability against dielectric breakdown. We estimate from this model that there should be $\sim 10^{20}$ chain-ends per cm^3 acting as defect sites in the linear PS chain melt compared to none in the cyclic PS melt.

In another recent study, we reported that the breakdown strength, E_{BD}, of the lamellae-forming pristine polystyrene-*block*-poly(methyl methacrylate) (PS-*b*-PMMA) block copolymer (BCP) was higher compared to that of the as-cast mixed disordered state of the homopolymers.[25,26] This was attributed to finite domain spacing, interface formation, and segregation of chain-ends with the BCP lamellae. The addition of block-specific linear homopolymer chains however showed that the BCP breakdown strength was compromised due to the increased free chain-ends introduced by the linear homopolymers, despite increased BCP domain spacing by the homopolymers.[26] Likewise, we then tested the ability of cyclic polymers rather than linear homopolymer additives, to

https://doi.org/10.1021/acspolymersau.2c00014
ACS Polym. Au 2022, 2, 324−332

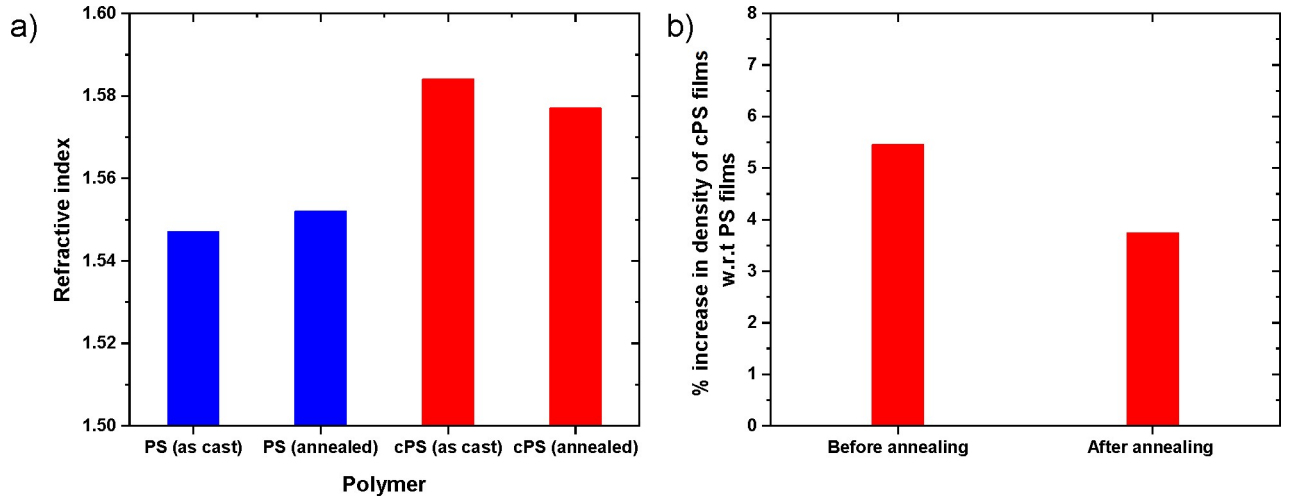

Figure 3. (a) Refractive indices of linear polystyrene (PS) films vs the cyclic polystyrene (cPS) films in the as-cast vs annealed films. (b) Calculated density difference of the cPS vs PS films using their refractive indices from ellipsometric measurements.

potentially enhance the system E_{BD} by virtue of increasing domain spacing without increasing chain-end density. Figures 2a–c shows the blend schematics for the blend film, the Weibull failure plots, and the E_{BD} for the blend films, respectively. The BCP + cPS blend films demonstrate ∼10% higher $E_{BD,}$ as compared to the BCP + PS blend films, with a similar 10 mass % addition of added polymer. The fact that the cyclic polymer additives enhance the breakdown strength E_{BD} of the BCP films, while in contrast the homopolymer additives lower the E_{BD} of the BCP films, confirms that the lack of chain-ends in cyclic polymers enhances the energy storage of BCP films.

The change of polymer architecture from linear to cyclic along with the absence of chain-ends may be expected to affect the packing density of the polymer films as well. Theoretically, it has been demonstrated that unknotted cyclic polymers pack tighter as compared to the linear polymers.[47] The Lorentz–Lorenz equation relates the polymer packing density and molecular parameters to the change in the refractive index of the polymer films,[48,49]

$$\frac{n^2 - 1}{n^2 + 1} = \frac{\alpha N_A}{3\varepsilon_0 M_0}\rho \tag{5}$$

Where n is the refractive index, ρ is the mass density, α is the molecular polarizability of the monomer repeat unit, N_A is Avogadro's number, ε_0 is the permittivity of free space, and M_0 is the monomer repeat unit molecular mass. Given that these quantities are the same in the PS and cPS, with the exception of the azide end-group, the Lorentz–Lorenz equation can be used to calculate the mass density of PS vs cPS. Figure 3a,b shows the refractive indices of the PS and cPS polymer films from ellipsometric measurements (Supporting Information Figure S5) and the calculated (using eq 5) change in the density of cPS vs. PS films in the as-cast and the annealed state. The density of cPS films is higher than that of PS films in both states. The density difference decreases in the annealed state, which might be due to more pronounced chain rearrangements of PS films during annealing. Interestingly, the dielectric strength of the as-cast cPS films is only ∼10% higher than the PS films (Supporting Information Figure S4), which might be due to the presence of the residual solvent or nonequilibrium chain packing. The enhanced density of the cPS films might be a contributing factor to the E_{BD} enhancement in cPS films.

Figure 4a,b shows the dielectric constant and the loss tangent for the PS and cPS polymers. The cPS shows a slightly higher dielectric constant in comparison to PS, but overall, the dielectric constant of cPS is lower as compared to many other polymers. The low dielectric constant of cPS, coupled with its high dielectric strength, makes it attractive for low-dielectric-constant material applications in the semiconductor industry.[50,51] Figure 4c,d shows the measured electric displacement vs. electric field for the PS and cPS polymer films. The electric displacement of PS and cPS varies linearly with the electric field strength, showing that both polymers exhibit a linear dielectric response. The PS shows efficiencies of 98 and 99% with remnant polarizations of 0.00086 and 0.0046 $\mu C/cm^2$ at 133 and 200 V/μm ($\sim E_{BD}$), respectively, while the cPS shows efficiencies of 99.6, 99, 95, and 94% and remnant polarizations of 0.0015, 0.0041, 0.0147, and 0.018 $\mu C/cm^2$ at 238, 272, 285, and 300 V/μm ($\sim E_{BD}$), respectively. Figure 4e shows the maximum charge per unit area stored in the PS and cPS polymers close to their E_{BD}. The cPS films can store higher charge as compared to the PS films due to their higher dielectric strength. The maximum discharge energy densities (U_d) for PS and cPS, calculated from the electric displacement vs. electric field loops (Supporting Information Figure S6), close to their E_{BD} are shown in Figure 4f. The U_d for cPS is ∼80% higher than that in the PS due to the higher dielectric strength of cPS. This enhancement in energy density by simple polymer topology manipulation is phenomenal and directly demonstrates the role of chain-ends in the performance of polymeric dielectric capacitors.

CONCLUSION

We have demonstrated that cyclic polystyrene shows enhanced dielectric strength and capacitive energy density as compared to its linear chain melt counterpart, an effect that is attributed to a relatively enhanced packing of the cyclic polymers relative to the linear chains of similar mass and chemistry, due to the absence of free chain-ends. In future work, it would be interesting to see the effect of cyclic polymer molar mass on the dielectric strength, with a hypothesis that the capacitive energy density would diminish upon increasing chain mass, an

https://doi.org/10.1021/acspolymersau.2c00014
ACS Polym. Au 2022, 2, 324–332

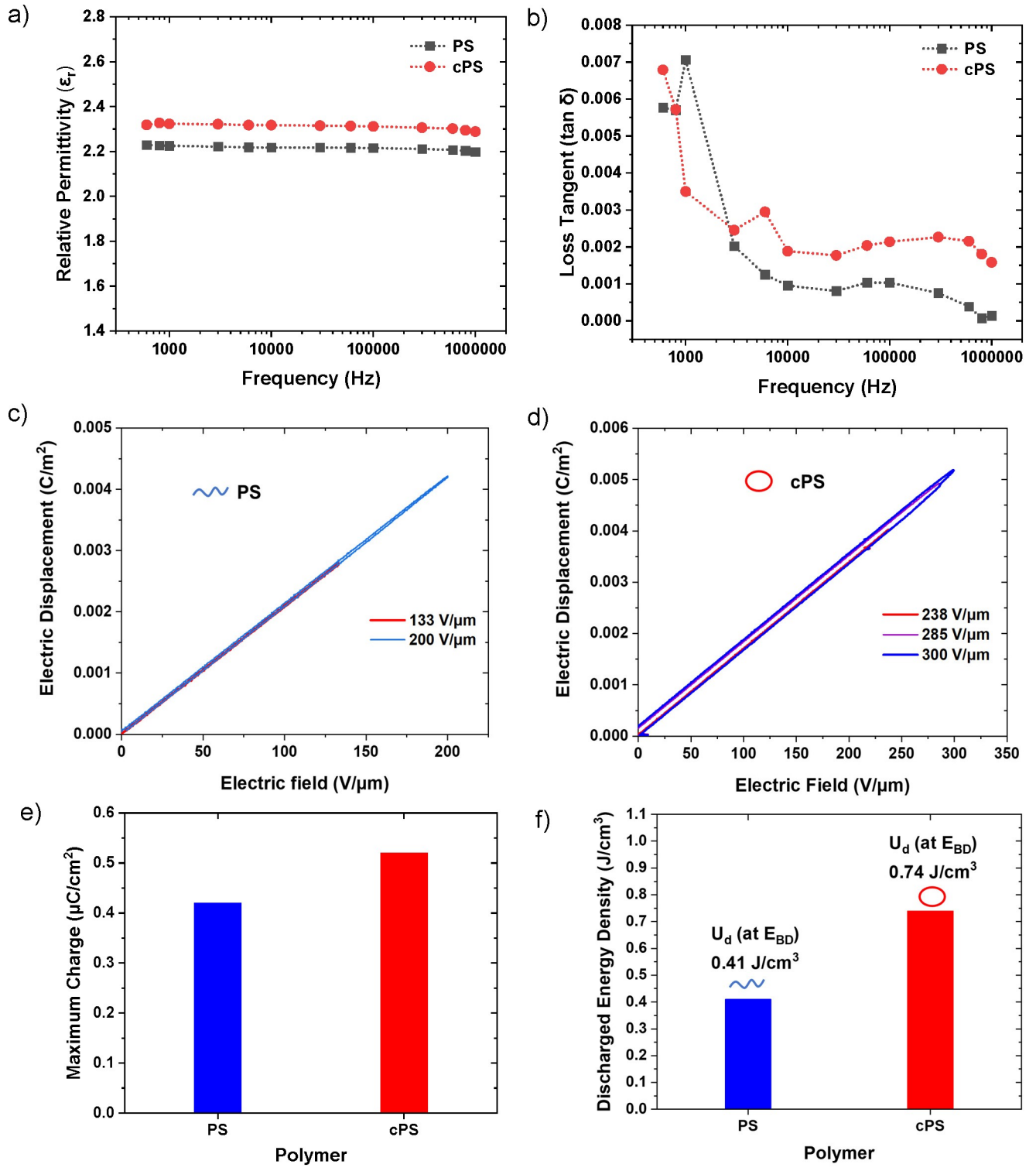

Figure 4. (a) Dielectric permittivity (ε_r) and (b) loss tangent (tan δ) as a function of frequency for linear polystyrene (PS) and cyclic polystyrene (cPS). (c) Electric displacement−electric field (D−E) loops of PS and (d) cPS at different electric fields. The D−E loops show linear behavior and very small remnant polarization for both PS and cPS. The D−E loops have been measured up to the polymer dielectric strength (E_{BD}). (e) Charge per unit area stored inside PS and cPS polymers near the E_{BD}. (f) Maximum discharge energy density (U_d) for PS and cPS. The maximum discharge energy density is ∼80% higher for cPS as compared to the PS.

expected effect since increasing mass decreases the density of free chain-ends. This simple free-volume argument has been applied for years to rationalize the decrease of mass dependence of glass transition with increasing molar mass.[52] We further note that the dielectric constant and refractive index of uncharged polymer materials depend strongly on the material density,[53] so we may expect that we can tune these, and other polymer properties that are strongly dependent on density (surface tension,[54] bulk modulus, melting temperature,[55] etc.) by simply altering the polymer topology. Finally,

https://doi.org/10.1021/acspolymersau.2c00014
ACS Polym. Au 2022, 2, 324−332

we note that the introduction of branching in polymer architecture leads to more complex changes to the density than just a decrease in the average polymer density associated with the additional free chain-ends.[42] Branching increases the density to an extent that depends strongly on branch functionality, but this effect is compensated by the reduction of the density arising from the chain-ends. Other polymer topologies including cyclic copolymers[56] and self-assembled cyclic polymers[57] should then be explored to determine if even greater enhancements of the resistance to dielectric breakdown can be achieved through the control of polymer molecular topology.

MATERIALS AND METHODS

Synthesis of Linear Polystyrene with Terminal Alkynyl and Bromo Alkyl Chain-Ends (Linear-PS-Br) (1)

To a flame-dried Schlenk flask, propargyl-2-bromoisobutyrate (40.3 mg, 0.197 mmol), styrene (2.2 mL, 19 mmol), *N*,*N*,*N*′,*N*″,*N*″-pentamethyldiethylenetriamine (PMDETA) (41.2 mg, 0.238 mmol), and anisole (∼2 mL) were added and degassed for three cycles of freeze−pump−thaw. After the third cycle, copper(I) bromide (CuBr) (29.3 mg, 0.203 mmol) was added to the reaction mixture. The flask was then resealed, evacuated, and refilled with N_2. The reaction mixture was allowed to warm to room temperature and stirred at 85 °C under N_2 for 7 h. After the reaction mixture was cooled in an ice bath, it was diluted with THF and passed through a column of neutral alumina to remove metal salts. The solution was then concentrated, and the crude product was precipitated into excess methanol to yield the polymer as a white solid (1.7 g, 85% yield). ^{1}H NMR (500 MHz, CD_2Cl_2, ppm) δ 7.34−6.88 (m, 210H, Ar$H_{meta/para}$), 6.88−6.34 (m, 130H, ArH_{ortho}), 4.61−4.38 (m, 1H, benzylicC$H_{bromide}$), 4.15−4.06 (m, 2H, propargylic CH_2O), 2.18−0.82 (m, 230H, alkynyl C*H*, isobutryl CH_3s, and backbone *H*s). ^{13}C NMR (126 MHz, CD_2Cl_2, ppm) 146.98−145.10, 129.81, 129.57−127.12, 126.67−125.55, 120.95, 78.52, 74.54, 41.61−40.45, 30.54. FT-IR(ATR): 3284, 3119−2751, 1828−1683, 1603, 1492, 1454, 1397−1261, 1211−1137, 1121, 1071, 1026, 989−884, 842, 758, 700 cm^{-1}. TGA in N_2, 320−440 °C, 96% mass loss. T_g = 90 °C. M_{nSEC} = 6.8 kDa, $Đ$ = 1.02.

Synthesis of Linear Polystyrene with a Terminal Alkyne and Azide Chain-Ends (Linear-PS-N_3) (2)

To a 100 mL round-bottom flask with a magnetic stir bar, **1** (150 mg, 25.0 μmol), NaN_3 (17.0 mg, 250 μmol) and 30 mL of DMF were added. The reaction mixture was allowed to stir at room temperature for 24 h. The resulting mixture was then precipitated into a large excess of methanol and washed with an excess amount of water and methanol. The white powder was collected by centrifugation and dried under vacuum overnight and gave a yield of 100 mg (62%). ^{1}H NMR (500 MHz, CD_2Cl_2, ppm) δ 7.37−6.91 (m, 180H, Ar$H_{meta/para}$), 6.91−6.28 (m, 120H, ArH_{ortho}), 4.16−3.87 (m, 3H, propargylic CH_2O and benzylicCH_{azide}), 2.54−0.73 (m, 200H, alkynyl C*H*, isobutryl CH_3s, and backbone *H*s). ^{13}C NMR (126 MHz, CD_2Cl_2, ppm) δ 147.15−145.13, 129.82, 129.25−127.31, 126.59−125.68, 120.96, 114.26, 55.49, 41.71−40.39. FT-IR(ATR): 3293, 3119−2766, 2635, 2344−2233, 2139−1992, 1736, 1687, 1603, 1501, 1450, 1115, 1121, 1068, 1032, 902, 754, 698 cm^{-1}. TGA in N_2, 320−440 °C, 100% weight loss. T_g = 91 °C. M_{nSEC} = 7.4 kDa, $Đ$ = 1.02.

Synthesis of Cyclic Polystyrene (cPS) (3)

Following the literature procedure,[45] to a 250 mL round-bottomed flask, PMDETA (0.5 g, 3 mmol) and 100 mL of anhydrous DMF were added and degassed for three cycles of freeze−pump−thaw. Next, CuBr (200 mg, 1.39 mmol) was added to the reaction mixture after the third cycle. The flask was then resealed, evacuated, and refilled with N_2. A separate flask containing Linear-PS-N_3 (90 mg, 15 μmol) dissolved in 5 mL of anhydrous DMF was degassed through two cycles of freeze−pump−thaw cycles. This solution was then added to the CuBr/PMDETA reaction solution dropwise at 120 °C via a syringe pump at a rate of 1 mL/h. Once addition of the polymer solution to the catalyst solution was complete, the reaction was allowed to proceed at 120 °C for an additional 12 h to ensure complete cyclization before allowing to cool to room temperature. The solvent was removed *in vacuo*, and the residue was diluted with chloroform. The remaining catalyst was removed by passing the chloroform solution of the reaction mixture through a neutral alumina column, and the solvent was removed *in vacuo*. The crude polymer was then dissolved in THF and precipitated in methanol to give a white powder (40 mg, 64%). ^{1}H NMR (500 MHz, CD_2Cl_2, ppm) δ 7.37−6.92 (m, 180H, Ar$H_{meta/para}$), 6.89−6.32 (m, 120H, ArH_{ortho}), 5.05 (m, 1H, benzylicC$H_{triazole}$), 4.53 (m, 2H, triazole-CH_2O), 2.60−0.62 (m, 220H, isobutryl CH_3s and backbone *H*s). ^{13}C NMR (126 MHz, CD_2Cl_2, ppm) δ 129.98−127.41, 126.82−125.40, 40.98−40.12. FT-IR(ATR): 3604−3273, 3130−2672, 1671, 1498, 1445, 1382, 1255, 1092, 1018, 755, 681 cm^{-1}. TGA in N_2, 25−277 °C, 20% weight loss, 280−420 °C, 80% weight loss. T_g = 102 °C. M_{nSEC} = 5.2 kDa, $Đ$ = 1.04. T_g = 102 °C.

Linear Polystyrene

The linear polystyrene (PS) used in this study was purchased from Polymer Source Inc. and has a product code of P40034−S. It has a molar mass of 6 kDa (similar to synthesized cPS used in this study) and dispersity of 1.10. Furthermore, PS from Polymer Source, Inc. was compared to Linear-PS-Br (**1**) (shown in the first step in Figure 1) used for the synthesis of cPS for the dielectric properties. The dielectric breakdown strength of the Linear-PS-N_3 (**2**) used for the synthesis of cPS is shown in Supporting Information Figure S3 and is close to that of the PS from polystyrene. This comparison further supplements the result that the dielectric strength enhancement of the cPS as compared to the PS is due to the cyclization and hence the missing chain-ends in the cPS films. The block copolymer polystyrene-*block*-poly(methyl methacrylate) (PS-*b*-PMMA) having a molar mass of 19.1-*b*-17.5 kDa was purchased from Polymer Source, Inc. All the polymers (synthesized as well as commercial) display white color in the powder form, indicating absence of any catalytic impurities.

Film Casting

The polymers (PS or cPS) were dissolved in toluene to make a 2% (mass/vol) solution. The solutions were drop-cast to generate ∼1−2 μm thick films on aluminum-coated silicon wafers or pure aluminum wafers. The aluminum electrodes (∼100 nm thickness) were deposited on silicon wafers using an ultrahigh-vacuum sputtering instrument. The silicon wafers were purchased from University Wafers. The pure aluminum wafers were also purchased from University Wafers. The polymer film thicknesses were measured locally using the atomic force microscopy (AFM) scratch test. The films were annealed at 80 °C for 15 h before electrical testing. The solutions for PS-*b*-PMMA and PS or cPS blend films were made by dissolving PS-*b*-PMMA in toluene and adding PS or cPS solution in desired quantities so that the homopolymer (PS or cPS) fraction was 10% with respect to the block copolymer. The blend films were flow-coated on aluminum-coated silicon wafers to yield thicknesses of ∼2.5 μm. The blend films were annealed at 210 °C for 24 h to induce block copolymer phase separation[58,59] and additive homopolymer segregation.

Optical Testing

For refractive index measurements, PS or cPS films with thickness ≈ 115−120 nm were flow-coated on silicon substrates to generate smooth films. Thinner films were used for refractive index measurements to lower the errors in the ellipsometry measurements, given that the surface roughness of thicker films contributes to errors in the refractive index measurements during ellipsometry. The measurements were performed using a J.A. Woolam Alpha-SE ellipsometer, and the data were fit using CompleteEASE software with B-spline model. The refractive indices are reported at a 632.8 nm wavelength. The mean squared errors were 1−2.2% during the fits. The measurements and the model fits are shown in Figure S5.

https://doi.org/10.1021/acspolymersau.2c00014
ACS Polym. Au 2022, 2, 324−332

Electrical Testing

The dielectric breakdown tests were performed using the PolyK testing system PK CPE-1801. The polymer films coated on aluminum-coated silicon wafers were contacted with a spring-loaded top electrode connected to the PolyK testing system, and the bottom aluminum electrode was connected to the ground. A ramp rate of 20 V/s was set for the dielectric testing, and the dielectric breakdown values were recorded using the PolyK software. For calculating the dielectric strength, ≈15 measurements were performed, and the data used two-parameter Weibull statics described as,

$$P(E) = 1 - \exp[-(E/E_{BD})^{\beta}]$$

where $P(E)$ is the cumulative probability of dielectric failure, E is the measured dielectric breakdown strength, E_{BD} is the Weibull dielectric strength, i.e., dielectric strength at 63% of the probability of failure, and β is the shape factor, which represents the reliability of the breakdown data. A higher β represents the higher reliability of the dielectric data.

For electrical displacement vs electric field loops ($D-E$ loops), the polymer films were drop-cast on the pure aluminum wafers. Top electrodes having a ∼0.3 mm diameter and ∼30 nm thickness were made by sputter coating gold using a desktop sputtering instrument. The top and bottom electrodes were connected to the instrument, and the $D-E$ loops were recorded using a unipolar triangular wave having 10 Hz frequency. The discharged energy density and the loss were calculated from the $D-E$ loops as demonstrated in Figure S6.

The frequency-dependent dielectric spectroscopy measurements were performed using the Keysight E4980 AL LCR meter. The films were coated on pure aluminum wafers, and the top electrodes were fabricated using eutectic Gallium−Indium liquid metal.

■ ASSOCIATED CONTENT

Supporting Information

The Supporting Information is available free of charge at https://pubs.acs.org/doi/10.1021/acspolymersau.2c00014.

NMR spectra, MALDI-ToF spectra of linear-PS-N_3 and cPS, dielectric strength of the PS-Br precursor used for the synthesis of cyclic polystyrene, dielectric strengths of as-cast PS and cPS films, ellipsometry data, and calculation of energy density from electric displacement vs electric field (PDF)

■ AUTHOR INFORMATION

Corresponding Author

Alamgir Karim − *Department of Chemical and Biomolecular Engineering, University of Houston, Houston, Texas 77204, United States;* orcid.org/0000-0003-1302-9374; Email: akarim3@central.uh.edu

Authors

Maninderjeet Singh − *Department of Chemical and Biomolecular Engineering, University of Houston, Houston, Texas 77204, United States;* orcid.org/0000-0001-8891-8454

Mei Dong − *Departments of Chemistry, Chemical Engineering, and Materials Science & Engineering, Texas A&M University, College Station, Texas 77842, United States;* orcid.org/0000-0002-9862-0296

Wenjie Wu − *Department of Chemical and Biomolecular Engineering, University of Houston, Houston, Texas 77204, United States*

Roushanak Nejat − *Materials Engineering Program, University of Houston, Houston, Texas 77204, United States*

David K. Tran − *Departments of Chemistry, Chemical Engineering, and Materials Science & Engineering, Texas A&M University, College Station, Texas 77842, United States;* orcid.org/0000-0002-4877-166X

Nihar Pradhan − *Department of Chemistry, Physics and Atmospheric Science, Jackson State University, Jackson, Mississippi 39217, United States;* orcid.org/0000-0002-3912-4233

Dharmaraj Raghavan − *Department of Chemistry, Howard University, Washington, DC 20059, United States;* orcid.org/0000-0002-7634-0656

Jack F. Douglas − *Materials Science and Engineering Division, National Institute of Standards and Technology, Gaithersburg, Maryland 20899, United States;* orcid.org/0000-0001-7290-2300

Karen L. Wooley − *Departments of Chemistry, Chemical Engineering, and Materials Science & Engineering, Texas A&M University, College Station, Texas 77842, United States*

Complete contact information is available at: https://pubs.acs.org/10.1021/acspolymersau.2c00014

Notes

The authors declare no competing financial interest.

Certain commercial equipment, instruments, or materials are identified in this paper in order to specify the experimental procedure accurately. Such identification is not intended to imply recommendation or endorsement by the National Institute of Standards and Technology nor is it intended to imply that the materials or equipment identified are necessarily the best available for the purpose.

■ ACKNOWLEDGMENTS

A.K., N.P., and D.R. acknowledge funding from NSF DMR # 1900692 for design of experiments, data interpretation, sample fabrication, electrical measurements, and characterization aspects of the work. K.L.W. acknowledges the National Science Foundation (DMR-1905818) and the Welch Foundation (A-0001) for support of the synthesis of cyclic polystyrene for the study. We also thank Dr. Guorong Sun for helpful discussions and careful review of the manuscript and Dr. Lu Su (Department of Chemistry, Texas A&M University) for helpful discussion and advice.

■ REFERENCES

(1) Koohi-Fayegh, S.; Rosen, M. A. A Review of Energy Storage Types, Applications and Recent Developments. *J. Energy Storage* **2020**, *27*, 101047.

(2) Pan, H.; Lan, S.; Xu, S.; Zhang, Q.; Yao, H.; Liu, Y.; Meng, F.; Guo, E. J.; Gu, L.; Yi, D.; Renshaw Wang, X. R.; Huang, H.; MacManus-Driscoll, J. L.; Chen, L. Q.; Jin, K. J.; Nan, C. W.; Lin, Y. H. Ultrahigh Energy Storage in Superparaelectric Relaxor Ferroelectrics. *Science* **2021**, *374* (6563), 100−104.

(3) Kim, J.; Saremi, S.; Acharya, M.; Velarde, G.; Parsonnet, E.; Donahue, P.; Qualls, A.; Garcia, D.; Martin, L. W. Ultrahigh Capacitive Energy Density in Ion-Bombarded Relaxor Ferroelectric Films. *Science* **2020**, *369* (6499), 81−84.

(4) Pan, H.; Li, F.; Liu, Y.; Zhang, Q.; Wang, M.; Lan, S.; Zheng, Y.; Ma, J.; Gu, L.; Shen, Y.; Yu, P.; Zhang, S.; Chen, L. Q.; Lin, Y. H.; Nan, C. W. Ultrahigh-energy Density Lead-Free Dielectric Films via Polymorphic Nanodomain Design. *Science* **2019**, *365* (6453), 578−582.

(5) Li, Q.; Chen, L.; Gadinski, M. R.; Zhang, S.; Zhang, G.; Li, H. U.; Iagodkine, E.; Haque, A.; Chen, L.-Q.; Jackson, T. N.; Wang, Q.

Flexible Higherature Dielectric Materials from Polymer Nanocomposites. *Nature* **2015**, *523* (7562), 576−579.
(6) Li, H.; Zhou, Y.; Liu, Y.; Li, L.; Liu, Y.; Wang, Q. Dielectric Polymers for High-Temperature Capacitive Energy Storage. *Chem. Soc. Rev.* **2021**, *50*, 6369.
(7) Prateek; Thakur, V. K.; Gupta, R. K. Recent Progress on Ferroelectric Polymer-Based Nanocomposites for High Energy Density Capacitors: Synthesis, Dielectric Properties, and Future Aspects. *Chem. Rev.* **2016**, *116* (7), 4260−4317.
(8) Palneedi, H.; Peddigari, M.; Hwang, G. T.; Jeong, D. Y.; Ryu, J. High-Performance Dielectric Ceramic Films for Energy Storage Capacitors: Progress and Outlook. *Adv. Funct. Mater.* **2018**, *28* (42), 1803665.
(9) Tan, D. Q. Review of Polymer-Based Nanodielectric Exploration and Film Scale-Up for Advanced Capacitors. *Adv. Funct. Mater.* **2020**, *30* (18), 1808567.
(10) Chu, B.; Zhou, X.; Ren, K.; Neese, B.; Lin, M.; Wang, Q.; Bauer, F.; Zhang, Q. M. A Dielectric Polymer with High Electric Energy Density and Fast Discharge Speed. *Science* **2006**, *313*, 334−336.
(11) Singh, M.; Apata, I.; Samant, S.; Wu, W.; Tawade, B.; Pradhan, N.; Raghavan, D.; Karim, A. Nanoscale Strategies to Enhance the Energy Storage Capacity of Polymeric Dielectric Capacitors: Review of Recent Advances. *Polym. Rev.* **2022**, *62*, 211.
(12) Zhu, L.; Wang, Q. Novel Ferroelectric Polymers for High Energy Density and Low Loss Dielectrics. *Macromolecules* **2012**, *45* (7), 2937−2954.
(13) Tawade, B. V.; Apata, I. E.; Singh, M.; Das, P.; Pradhan, N.; Al-Enizi, A. M.; Karim, A.; Raghavan, D. Recent Developments in the Synthesis of Chemically Modified Nanomaterials for Use in Dielectric and Electronics Applications. *Nanotechnology* **2021**, *32* (14), 142004.
(14) Rao, Y. L.; Chortos, A.; Pfattner, R.; Lissel, F.; Chiu, Y. C.; Feig, V.; Xu, J.; Kurosawa, T.; Gu, X.; Wang, C.; He, M.; Chung, J. W.; Bao, Z. Stretchable Self-Healing Polymeric Dielectrics Cross-Linked through Metal-Ligand Coordination. *J. Am. Chem. Soc.* **2016**, *138* (18), 6020−6027.
(15) Jiang, B.; Iocozzia, J.; Zhao, L.; Zhang, H.; Harn, Y. W.; Chen, Y.; Lin, Z. Barium Titanate at the Nanoscale: Controlled Synthesis and Dielectric and Ferroelectric Properties. *Chem. Soc. Rev.* **2019**, *48* (4), 1194−1228.
(16) Stefanescu, E. A.; Tan, X.; Lin, Z.; Bowler, N.; Kessler, M. R. Multifunctional PMMA-Ceramic Composites as Structural Dielectrics. *Polymer (Guildf).* **2010**, *51* (24), 5823−5832.
(17) Guo, H. Z.; Mudryk, Y.; Ahmad, M. I.; Pang, X. C.; Zhao, L.; Akinc, M.; Pecharsky, V. K.; Bowler, N.; Lin, Z. Q.; Tan, X. Structure Evolution and Dielectric Behavior of Polystyrene-Capped Barium Titanate Nanoparticles. *J. Mater. Chem.* **2012**, *22* (45), 23944−23951.
(18) Grabowski, C. A.; Fillery, S. P.; Westing, N. M.; Chi, C.; Meth, J. S.; Durstock, M. F.; Vaia, R. A. Dielectric Breakdown in Silica-Amorphous Polymer Nanocomposite Films: The Role of the Polymer Matrix. *ACS Appl. Mater. Interfaces* **2013**, *5* (12), 5486−5492.
(19) Fillery, S. P.; Koerner, H.; Drummy, L.; Dunkerley, E.; Durstock, M. F.; Schmidt, D. F.; Vaia, R. A. Nanolaminates: Increasing Dielectric Breakdown Strength of Composites. *ACS Appl. Mater. Interfaces* **2012**, *4* (3), 1388−1396.
(20) Wang, Q.; Zhu, L. Polymer Nanocomposites for Electrical Energy Storage. *J. Polym. Sci., Part B: Polym. Phys.* **2011**, *49* (20), 1421−1429.
(21) Paniagua, S. A.; Kim, Y.; Henry, K.; Kumar, R.; Perry, J. W.; Marder, S. R. Surface-Initiated Polymerization from Barium Titanate Nanoparticles for Hybrid Dielectric Capacitors. *ACS Appl Mater Interfaces* **2014**, *6*, 3477−3482.
(22) Baer, E.; Zhu, L. 50th Anniversary Perspective: Dielectric Phenomena in Polymers and Multilayered Dielectric Films. *Macromolecules* **2017**, *50* (6), 2239−2256.
(23) Mackey, M.; Schuele, D. E.; Zhu, L.; Flandin, L.; Wolak, M. A.; Shirk, J. S.; Hiltner, A.; Baer, E. Reduction of Dielectric Hysteresis in Multilayered Films via Nanoconfinement. *Macromolecules* **2012**, *45* (4), 1954−1962.
(24) Artbauer, J. Electric Strength of Polymers. *J. Phys. D. Appl. Phys.* **1996**, *29* (2), 446−456.
(25) Samant, S. P.; Grabowski, C. A.; Kisslinger, K.; Yager, K. G.; Yuan, G.; Satija, S. K.; Durstock, M. F.; Raghavan, D.; Karim, A. Directed Self-Assembly of Block Copolymers for High Breakdown Strength Polymer Film Capacitors. *ACS Appl. Mater. Interfaces* **2016**, *8* (12), 7966−7976.
(26) Samant, S.; Basutkar, M.; Singh, M.; Masud, A.; Grabowski, C. A.; Kisslinger, K.; Strzalka, J.; Yuan, G.; Satija, S.; Apata, I.; Raghavan, D.; Durstock, M.; Karim, A. Effect of Molecular Weight and Layer Thickness on the Dielectric Breakdown Strength of Neat and Homopolymer Swollen Lamellar Block Copolymer Films. *ACS Appl. Polym. Mater.* **2020**, *2* (8), 3072−3083.
(27) Haque, F. M.; Grayson, S. M. The Synthesis, Properties and Potential Applications of Cyclic Polymers. *Nat. Chem.* **2020**, *12* (5), 433−444.
(28) Liénard, R.; De Winter, J.; Coulembier, O. Cyclic Polymers: Advances in Their Synthesis, Properties, and Biomedical Applications. *J. Polym. Sci.* **2020**, *58* (11), 1481−1502.
(29) KRICHELDORF, H. R. Cyclic Polymers: Synthetic Strategies and Physical Properties. *J. Polym. Sci. Part A Polym. Chem.* **2010**, *48* (April), 251−284.
(30) Bielawski, C. W.; Benitez, D.; Grubbs, R. H. An "Endless" Route to Cyclic Polymers. *Science* **2002**, *297* (5589), 2041−2044.
(31) Kapnistos, M.; Lang, M.; Vlassopoulos, D.; Pyckhout-Hintzen, W.; Richter, D.; Cho, D.; Chang, T.; Rubinstein, M. Unexpected Power-Law Stress Relaxation of Entangled Ring Polymers. *Nat. Mater.* **2008**, *7* (12), 997−1002.
(32) Nasongkla, N.; Chen, B.; Macaraeg, N.; Fox, M. E.; Fréchet, J. M. J.; Szoka, F. C. Dependence of Pharmacokinetics and Biodistribution on Polymer Architecture: Effect of Cyclic versus Linear Polymers. *J. Am. Chem. Soc.* **2009**, *131* (11), 3842−3843.
(33) Zhang, K.; Lackey, M. A.; Cui, J.; Tew, G. N. Gels Based on Cyclic Polymers. *J. Am. Chem. Soc.* **2011**, *133* (11), 4140−4148.
(34) Zhang, L.; Elupula, R.; Grayson, S. M.; Torkelson, J. M. Major Impact of Cyclic Chain Topology on the Tg-Confinement Effect of Supported Thin Films of Polystyrene. *Macromolecules* **2016**, *49* (1), 257−268.
(35) Zhang, L.; Elupula, R.; Grayson, S. M.; Torkelson, J. M. Suppression of the Fragility-Confinement Effect via Low Molecular Weight Cyclic or Ring Polymer Topology. *Macromolecules* **2017**, *50* (3), 1147−1154.
(36) Xu, J.; Ye, J.; Liu, S. Synthesis of Well-Defined Cyclic Poly(N-Isopropylacrylamide) via Click Chemistry and Its Unique Thermal Phase Transition Behavior. *Macromolecules* **2007**, *40* (25), 9103−9110.
(37) Jiang, N.; Chen, J.; Yu, T.; Chao, A.; Kang, L.; Wu, Y.; Niu, K.; Li, R.; Fukuto, M.; Zhang, D. Cyclic Topology Enhancing Structural Ordering and Stability of Comb-Shaped Polypeptoid Thin Films against Melt-Induced Dewetting. *Macromolecules* **2020**, *53* (17), 7601−7612.
(38) Kelly, G. M.; Haque, F. M.; Grayson, S. M.; Albert, J. N. L. Suppression of Melt-Induced Dewetting in Cyclic Poly(ϵ-Caprolactone) Thin Films. *Macromolecules* **2017**, *50* (24), 9852−9856.
(39) Córdova, M. E.; Lorenzo, A. T.; Müller, A. J.; Hoskins, J. N.; Grayson, S. M. A Comparative Study on the Crystallization Behavior of Analogous Linear and Cyclic Poly(ε-Caprolactones). *Macromolecules* **2011**, *44* (7), 1742−1746.
(40) Kawaguchi, D. Direct Observation and Mutual Diffusion of Cyclic Polymers. *Polym. J.* **2013**, *45* (8), 783−789.
(41) White, R. P.; Lipson, J. E. G. Free Volume in the Melt and How It Correlates with Experimental Glass Transition Temperatures: Results for a Large Set of Polymers. *ACS Macro Lett.* **2015**, *4* (5), 588−592.
(42) Chremos, A.; Douglas, J. F. Communication: When Does a Branched Polymer Become a Particle? *J. Chem. Phys.* **2015**, *143* (11), 111104.

https://doi.org/10.1021/acspolymersau.2c00014
ACS Polym. Au 2022, 2, 324−332

(43) Niu, W.; Gonsales, S. A.; Kubo, T.; Bentz, K. C.; Pal, D.; Savin, D. A.; Sumerlin, B. S.; Veige, A. S. Polypropylene: Now Available without Chain Ends. *Chem.* **2019**, *5* (1), 237−244.
(44) Bielawski, C. W.; Benitez, D.; Grubbs, R. H. Synthesis of Cyclic Polybutadiene via Ring-Opening Metathesis Polymerization: The Importance of Removing Trace Linear Contaminants. *J. Am. Chem. Soc.* **2003**, *125* (28), 8424−8425.
(45) Laurent, B. A.; Grayson, S. M. An Efficient Route to Well-Defined Macrocyclic Polymers via "Click" Cyclization. *J. Am. Chem. Soc.* **2006**, *128* (13), 4238−4239.
(46) Gao, L.; Oh, J.; Chang, T.; Chen, D.; Li, X.; Yang, X.; Tu, Y.; Zhu, X.; Li, C. Y. A Nearly Quantitative Synthetic Approach towards Monocyclic Polystyrenes and the Solvent, Concentration and Molecular Weight Effect on Cyclic Yield. *Polymer (Guildf).* **2016**, *101*, 379−387.
(47) Chremos, A.; Douglas, J. F. A Comparative Study of Thermodynamic, Conformational, and Structural Properties of Bottlebrush with Star and Ring Polymer Melts. *J. Chem. Phys.* **2018**, *149* (4), 044904.
(48) Han, Y.; Huang, X.; Rohrbach, A. C. W.; Roth, C. B. Comparing Refractive Index and Density Changes with Decreasing Film Thickness in Thin Supported Films across Different Polymers. *J. Chem. Phys.* **2020**, *153* (4), 044902.
(49) Vignaud, G.; Chebil, M. S.; Bal, J. K.; Delorme, N.; Beuvier, T.; Grohens, Y.; Gibaud, A. Densification and Depression in Glass Transition Temperature in Polystyrene Thin Films. *Langmuir* **2014**, *30* (39), 11599−11608.
(50) Volksen, W.; Miller, R. D.; Dubois, G. Low Dielectric Constant Materials. *Chem. Rev.* **2010**, *110*, 56−110.
(51) Yang, S.; Mirau, P. A.; Pai, C. S.; Nalamasu, O.; Reichmanis, E.; Pai, J. C.; Obeng, Y. S.; Seputro, J.; Lin, E. K.; Lee, H. J.; Sun, J.; Gidley, D. W. Nanoporous Ultralow Dielectric Constant Organosilicates Templated by Triblock Copolymers. *Chem. Mater.* **2002**, *14* (1), 369−374.
(52) Fox, T. G.; Flory, P. J. Second-Order Transition Temperatures and Related Properties of Polystyrene. I. Influence of Molecular Weight. *J. Appl. Phys.* **1950**, *21* (6), 581−591.
(53) Panuganti, S. R.; Vargas, F. M.; Chapman, W. G. Property Scaling Relations for Nonpolar Hydrocarbons. *Ind. Eng. Chem. Res.* **2013**, *52* (23), 8009−8020.
(54) Sauer, B. B.; Dee, G. T. Molecular Weight and Temperature Dependence of Polymer Surface Tension: Comparison of Experiment with Theory. *Macromolecules* **1991**, *24*, 2124−2126.
(55) Chickos, J. S.; Nichols, G. Simple Relationships for the Estimation of Melting Temperatures of Homologous Series. *J. Chem. Eng. Data* **2001**, *46* (3), 562−573.
(56) Nicolaÿ, R.; Matyjaszewski, K. Synthesis of Cyclic (Co)-Polymers by Atom Transfer Radical Cross-Coupling and Ring Expansion by Nitroxide-Mediated Polymerization. *Macromolecules* **2011**, *44* (2), 240−247.
(57) Williams, R. J.; Dove, A. P.; O'Reilly, R. K. Self-Assembly of Cyclic Polymers. *Polym. Chem.* **2015**, *6* (16), 2998−3008.
(58) Singh, M.; Agrawal, A.; Wu, W.; Masud, A.; Armijo, E.; Gonzalez, D.; Zhou, S.; Terlier, T.; Zhu, C.; Strzalka, J.; Matyjaszewski, K.; Bockstaller, M.; Douglas, J. F.; Karim, A. Soft-Shear-Aligned Vertically Oriented Lamellar Block Copolymers for Template-Free Sub-10 nm Patterning and Hybrid Nanostructures. *ACS Appl. Mater. Interfaces* **2022**, *14* (10), 12824−12835.
(59) Wu, W.; Singh, M.; Masud, A.; Wang, X.; Nallapaneni, A.; Xiao, Z.; Zhai, Y.; Wang, Z.; Terlier, T.; Bleuel, M.; Yuan, G.; Satija, S. K.; Douglas, J. F.; Matyjaszewski, K.; Bockstaller, M. R.; Karim, A. Control of Phase Morphology of Binary Polymer Grafted Nanoparticle Blend Films via Direct Immersion Annealing. *ACS Nano* **2021**, *15* (7), 12042−12056.

https://doi.org/10.1021/acspolymersau.2c00014
ACS Polym. Au 2022, 2, 324−332